

Influence of climatic changes on oceanographic properties of the Adriatic Sea

Branka GRBEC

Institute of Oceanography and Fisheries, P.O.Box 500, 21000 Split, Croatia

In order to explain possible influence of climatic changes on the oceanographic properties of the Adriatic Sea, available historic datasets (hydrographic, sea level and meteorological ones) are studied. Three important time scales are investigated separately: secular, interannual and seasonal. At a secular time scale, basic climatic oscillation was determined analysing long-term records of meteorological and sea level data for the Trieste station. Interannual variations of sea surface temperature and sea level along the eastern Adriatic coast as well as data series of temperature and salinity for the vertical profile in the open middle Adriatic were described using the correlation matrix based principal component analysis. The results were compared to the conditions in the atmosphere, leading to the conclusion that changes in atmospheric pressure account for a significant part of low frequency sea level changes. Additionally, thermohaline fluctuations in the surface layer were correlated with the atmospheric forcing, while the intermediate layer responded to the pressure gradient between the northern and southern Adriatic. At a seasonal scale, thermohaline fluctuations (described in terms of the principal component scores) in comparison to the heat and water fluxes point to the fact that atmosphere strongly affects the seawater properties of the surface layer. In this layer, temperature and salinity vertical gradients are well related to the surface fluxes all the year round. In deeper layers this influence is observed only under vertically homogenous conditions. From heat and salt balances in this layer, it follows that two different seasons could be distinguished: a cold season with important vertical processes and a warm season with prevailing horizontal exchanges.

INTRODUCTION

There are several reasons why the Adriatic Sea is a suitable area for studies of possible influence of climatic changes on the oceanographic properties. The most important reason is the long-term dataset of hydrographic measurements.

The earliest research of the Adriatic Sea dates back to the past century. However, systematic and regular measurements in the middle and southern Adriatic began in the 1950s (BULJAN and ZORE-ARMANDA, 1976,

1979; ZORE-ARMANDA *et al.*, 1991). The best investigated area is the transect Split-Gargano in the middle Adriatic, which is a region with a strong temporal variability of thermohaline structure caused by seasonally dependent circulation. This area is exposed to influences from both the northern and the southern Adriatic. The dynamics of the study transect is also controlled by the topographic effect on the Palagruža Sill (ZORE-ARMANDA and BONE, 1987). A comprehensive review paper on the dynamics of the Adriatic Sea is given in the work by ORLIĆ *et al.* (1992). Generally,

current flows from the Adriatic into the Mediterranean in the surface and bottom layers, while the Mediterranean water enters the Adriatic in intermediate layer. In winter, in the northern Adriatic, very cold dense water is formed, which sinks to deep layers of the Jabuka Pit, and is advected across the Palagruža Sill (ZORE-ARMANDA, 1963). The transect area is also under the influence of saltier water advected from the southern Adriatic. The most important feature of the Mediterranean waters advecting into the Adriatic (in the intermediate layer) is their high salinity (BULJAN and ZORE-ARMANDA, 1976). This high salinity is a property of the Levantine Basin, which has one of the highest salinity rates among the world oceans (>39 psu) (MORCOS, 1972; TZIPERMAN AND MALANOTTE-RIZZOLI, 1991). Advection of the Mediterranean water, called "ingression" (BULJAN, 1953), carries Mediterranean saltier water into the Adriatic, causing a strong increase in salinity in the middle Adriatic. Since the temperature of Levantine intermediate water (LIW) is higher than that of the Adriatic water, "ingressions" are reflected upon the temperature as well (ZORE-ARMANDA, 1969a). Additionally, ingressions also cause an increase in nutrients which enhance production (BULJAN, 1964, 1974; PUCHER-PETKOVIĆ and ZORE-ARMANDA, 1973). Relating these phenomena to the climate, ZORE-ARMANDA (1969b, 1991) stated that the most important factor enhancing the water exchange between the two basins is the horizontal pressure gradient over the eastern Mediterranean. At the same time, the location of the Icelandic cyclone and the Siberian anticyclone centers were found responsible for pressure differences (ZORE-ARMANDA 1969c, 1972). It was observed that such changes could be related to the conditions of a wide area of the northern Atlantic and Europe (ZORE-ARMANDA, 1974). An increasing trend was observed in horizontal pressure gradient over the Adriatic, causing increasing trend of salinity in the intermediate layer in the middle Adriatic (ZORE-ARMANDA, 1969b). It is therefore suggested

that the impact of climatic change could play an important role in long-term trends in hydrographic properties of the Adriatic Sea.

This paper attempts to describe long-term changes of relevant meteorological parameters and to relate these changes to oceanographic parameters. The outline of the paper is as follows. Methodology section introduces various methods such as: trend analysis, basic climatic oscillation, principal component analysis (PCA) and heat and salt balances analysis. The analysis is performed on three time scales. Data section provides a historical dataset. Next section discussed the application of the analyses performed in research. Results obtained by this methodology are related to fluctuations of heat and water fluxes at the air-sea interface for both interannual and seasonal time scales. A particular attention was paid to the surface water flux, since it determines vertical eddy diffusion coefficients. Conclusions are presented in the last section.

METHODOLOGY

Trend analysis and basic climatic oscillation

Basic climatic oscillation was determined using the function of the first harmonic:

$$y(t) = a_0 + a_1 t + a_2 \sin\left(\frac{2\pi t}{T} + \psi\right), \quad (1)$$

where $a_0 + a_1 t$ denotes linear trend, a_2 and ψ amplitude and phase of first harmonic. In order to eliminate seasonal cycle from input data x_t , monthly mean values were filtered using symmetric digital filter :

$$y_t = \sum_{k=-n}^n w_k x_{t+k}, \quad w_{-k} = w_k. \quad (2)$$

For the weights (w_k), values of 24m214 filter (THOMPSON, 1983) was chosen. The filter is

symmetric, so the total length is 49 (48 months).

The basic climatic oscillation (1) allowed to determine the role trend and/or oscillation for the description of data series, depending on significance of particular terms in equation (1).

Principal component analysis

Principal component analysis (PCA) (PREISENDORFER, 1982) was used to analyse spatial and temporal variability of sea level and sea surface temperatures and to describe the vertical structure of seawater temperature and salinity. The PCA attempts to find a relatively small number of independent quantities (factors or principal components) which convey as much of the original information as possible without redundancy. Instead of a large number of initially, nonorthogonal (manifest) variables the dataset containing a small number of orthogonal (latent) variables is given. It is then possible to use a small number of principal components instead of a large number of original variables. The most important property of principal components is that they are orthogonal, namely, the correlation between any two different components is zero.

The PCA was performed on the correlation matrix of standardised variables $z_k(i)$ of observation vectors $\mathbf{X}(i)$:

$$z_k(i) = \frac{x_k(i) - \bar{x}(i)}{\sigma_x(i)} \quad (3)$$

$k = 1, 2, \dots, n; i = 1, 2, \dots, N.$

Correlation matrix is:

$$R_{ij} = \frac{1}{n} \sum_{k=1}^n z_k(i) z_k(j) \quad (4)$$

$i, j = 1, 2, \dots, N,$

or in the matrix notation:

$$\mathbf{R} = n^{-1} (\mathbf{Z}\mathbf{Z}^T) \quad (5)$$

where T denotes the transpose.

Principal component analysis (or any other factor analysis) is used only if the correlation matrix of the original variables is significant. In order to test the significance of the correlation matrix, the BARTLETT test (FULGOSI, 1988) with s degree of freedom was used:

$$\chi^2(s) = -\left(n-1 - \frac{2N+5}{6}\right) \ln|\mathbf{R}|, \quad (6)$$

$$s = N \frac{N-1}{2},$$

where n denotes the number of data, N the number of variables and $|\mathbf{R}|$ the determinant of the correlation matrix. The determinant of the correlation matrix is a product of eigenvalues:

$$|\mathbf{R}| = \lambda_1 \cdot \lambda_2 \cdot \dots \cdot \lambda_N. \quad (7)$$

If quantity $\chi^2(s)$ exceeds a particular level of significance of χ^2 -test, then the application of PCA to the matrix \mathbf{R} is justified.

As it is known from linear algebra, a real symmetric matrix (in our case matrix \mathbf{R}) has only real eigenvalues and there exists a real orthogonal matrix Φ so that $\Phi^{-1}\mathbf{R}\Phi$ is diagonal. The diagonal elements are then eigenvalues and the columns are the eigenvectors. Eigenvalues and eigenvectors were determined as a solution of matrix equation:

$$\Phi^{-1}\mathbf{R}\Phi = \lambda \quad (8)$$

The solution of matrix equation is obtained using iterative JACOBI's method (SPIEGEL, 1972). In JACOBI's method, the solution of equation (8) is completed after obtaining a finite product of "rotations" of matrices of the form:

$$\Phi_1 = \begin{bmatrix} \cos\alpha & -\sin\alpha \\ \sin\alpha & \cos\alpha \end{bmatrix} \quad (9)$$

All other elements in matrix Φ_1 are identical with those of the unit matrix. If the four entries

in equation (9) are in positions (i,i) , (i,k) , (k,i) and (k,k) and choosing such a transformation angle that:

$$\tan 2\alpha_{ik} = \frac{2r_{ik}}{r_{ii} - r_{kk}}, \quad (10)$$

corresponding elements of $\Phi^{-1}\mathbf{R}\Phi$ may easily be computed. Each step of the JACOBI algorithm makes a pair of off-diagonal elements equal zero. Successive matrices of this form approach the required diagonal form. The diagonalization on \mathbf{R} is therefore performed by stepwise orthogonal transformation, each step of the form:

$$\begin{aligned} \Phi_1^{-1}\mathbf{R}\Phi_1 &= \mathbf{R}_1, \\ \Phi_2^{-1}\mathbf{R}_1\Phi_2 &= \mathbf{R}_2, \\ \Phi_g^{-1}\mathbf{R}_{g-1}\Phi_g &= \mathbf{R}_g = \mathbf{E}. \end{aligned} \quad (11)$$

After g rotations this procedure approaches the diagonal matrix form. The column of \mathbf{E} has been arranged in such a way that λ_1 is the largest eigenvalue of \mathbf{R} , λ_2 the next largest value of \mathbf{R} , and so forth. The same procedure has been performed for matrix Φ of eigenvectors. After the solutions of eigenvalues and eigenvectors are found, the factor matrix of component loadings can be determined:

$$\mathbf{F} = \Phi \mathbf{E}_r^{1/2}, \quad (12)$$

where r is the number of factors (principal components) taken into consideration. The dimension of matrices \mathbf{F} and Φ are $(N \times r)$.

In order to find out how much of the variance of the original field is accounted for by principal components, the value $Pr = (\lambda_r / N) 100\%$ is determined, where the individual variance is determined by the eigenvalue:

$$V_r = \frac{\sum_{i=1}^r \lambda_i}{\sum_{i=1}^N \lambda_i} \quad (13)$$

The sum of the P_r show how much of the original variance has been explained by the r principal components. The significance of principal components were tested with Rule N* (OVERLAND and PREISENDORFER, 1982), using Monte Carlo simulation of the random matrix of the same size as the original data matrix.

After the above procedure, initial correlation matrix of standardised variables \mathbf{R} is presented by $(N \times r)$ factor matrix of component loadings \mathbf{F} and diagonal matrix of r eigenvalues \mathbf{E} , while initial vector of manifest variables can be expressed as a linear combination of r eigenvectors:

$$k_k(i) = \mathbf{F}^{-1} \cdot z_k(i), \quad i = 1, \dots, n; k = 1, \dots, N \quad (14)$$

The $z_k(i)$ observations refer to n different times and, therefore, $k_k(i)$ represents time variation of the coefficient (PC score) associated with the eigenvector.

In most applications of PC techniques, a large portion of variance can be accounted for by retaining only the first few eigenvalues (first few principal components). In that case the first few terms (r components) only approximate the observation vectors, e.g. a large fraction of the total variance is explained by small number of eigenvectors.

Another important part of the technique described above is the possibility of rotation in PC coordinate frame. A rotation of PCs can be useful for offering a better insight into the behavior of observation variables. In most of the analyses, unrotated PCs are difficult to interpret (in sense of physical causes). In order to achieve a simple structure (RICHMANN,

* Rule N compares the eigenvalues obtained from real data matrix with those obtained from random data matrix. Those eigenvalues from real data matrix which describe an equal or smaller percentage of total variance than corresponding eigenvalues obtained from random data matrix are not significant.

1986) rotation is therefore commonly used. Varimax rotation was applied in this work. A more detailed discussion of rotation can be found in FULGOSI (1988).

Heat and salt balance equations

Temperature and salinity variations are governed by the heat and salt balance equations:

$$\rho_w c_{pw} \frac{\partial T}{\partial t} = \frac{\partial H_{ver}}{\partial z} + \frac{\partial H_{hor}}{\partial y} \quad (15)$$

$$\rho_w \beta \frac{\partial s}{\partial t} = \frac{\partial S_{ver}}{\partial z} + \frac{\partial S_{hor}}{\partial y}$$

Horizontal component of heat and salt fluxes (H_{hor} , S_{hor}) include both advective and diffusive effects and cannot be calculated with data from the Split-Gargano transect alone. Neglecting convection, the vertical part between surface ($z=0$) and a bottom reference level ($z=-h$) is:

$$\int_{-h}^0 \frac{\partial T}{\partial t} dz = \int_{-h}^0 \frac{\partial}{\partial z} (K_H \frac{\partial T}{\partial z}) dz \quad (16)$$

$$\int_{-h}^0 \frac{\partial s}{\partial t} dz = \int_{-h}^0 \frac{\partial}{\partial z} (K_S \frac{\partial s}{\partial z}) dz$$

Using parametrisation:

$$H_{ver} = \begin{cases} Q_{NET} & z = 0 \\ K_H \rho_w c_{pw} \frac{\partial T}{\partial z} & z < 0, \end{cases} \quad (17)$$

$$S_{ver} = \begin{cases} \rho_w \beta s_0 (E - P) & z = 0 \\ K_S \rho_w \beta \frac{\partial s}{\partial z} & z < 0, \end{cases}$$

it was possible to determine vertical heat and salt fluxes and their seasonal rate of change

caused by vertical processes. From heat and salt balance equations difference between total rate of change of heat and salt content on the one hand, and the rate caused by vertical processes, is attributed to horizontal processes.

In order to calculate vertical change of heat and salt it was necessary to determine vertical eddy diffusion coefficients for temperature and salinity (K_H and K_S) in the surface layer. Using the boundary conditions in the finite difference form and temperature and salinity at surface and at 10 m depth, it was possible to determine vertical eddy diffusion coefficients K_H and K_S on the basis of climatological data.

In order to smooth seasonal variability, represented by data from different years and different stations, the function of the form:

$$Y_z(t) = A_0 + A_1 \sin\left(\frac{2\pi}{T}t + \phi_1\right) + A_2 \sin\left(\frac{4\pi}{T}t + \phi_2\right), \quad (18)$$

was least-square fitted to data at seasonal scale for every depth z . The same function was fitted to PC scores which resulted in the loss of orthogonality. It was not possible to approximate salinity data by a harmonic function, so that salinity means were determined by averaging inside months. Fluctuations in the field of temperature and salinity were compared to the fluctuations of the processes at the air-sea interface. Harmonic analysis was applied to most of the data in order to compare temperature fluctuations to the processes at the air-sea interface. When comparing atmospheric and salinity data, monthly mean values were taken.

DATA

The meteorological dataset

The mean monthly meteorological dataset used in this work includes air temperature, wind speed, air humidity, air pressure, precipitation and sea surface temperature (Tables 1 and 2) at stations along the eastern Adriatic

Table 1. Meteorological dataset

STATION	METEOROLOGICAL PARAMETERS	PERIOD OF MEASUREMENT	SOURCE
TRIESTE	AIR TEMPERATURE	1841-1991	ISTITUTO TALASSOGRAFICO - TRIESTE
	AIR PRESSURE		
	PRECIPITATION	1871-1991	
	HUMIDITY		
	WIND SPEED		
EVAPORATION			
SENJ SPLIT HVAR DUBROVNIK PALAGRUŽA	AIR TEMPERATURE AIR PRESSURE PRECIPITATION HUMIDITY WIND SPEED EVAPORATION	1961-1980	NATIONAL HIDRO- METEOROLOGICAL OFFICE - ZAGREB

Table 2. Sea surface temperature dataset

STATION	SEA SURFACE TEMPERATURE	PERIOD OF MEASUREMENT	SOURCE
TRIESTE	SEA SURFACE TEMPERATURE AT 200 cm	1934-1991	ISTITUTO TALASSOGRAFICO - TRIESTE
	SEA SURFACE TEMPERATURE AT 40 cm	1988	
PIRAN RAB SENJ SPLIT HVAR DUBROVNIK	SEA SURFACE TEMPERATURE	1961-1980	NATIONAL HIDRO- METEOROLOGICAL OFFICE - ZAGREB

coast (Fig.1). Using this dataset, surface heat and water fluxes were determined.

Net heat exchange (Q_{NET}) in the air-sea interface is a sum of radiative and turbulent fluxes. The radiative component of the heat fluxes comprises solar (Q_S) and upward long-wave (Q_L) components. Turbulent heat fluxes are sensible (Q_H) and latent (Q_E) heat fluxes. All heat exchanges are calculated using monthly means values of bulk variables (for Hvar station) following GILL (1982):

$$\begin{aligned}
 Q_S &= Q'_s(1-\alpha), \\
 Q_L &= -0.985 \sigma T_w^4 (0.39 - 0.05e^{1/2})(10 - 0.06C^2), \\
 Q_E &= -LE, \\
 Q_H &= C_H c_p \rho_a v (T_a - T_w).
 \end{aligned}
 \tag{19}$$

where Q'_s is the incoming shortwave radiation and α is the albedo of the sea surface. The meanings of other terms in the above equations are given in Appendix.

The monthly means of shortwave radiation were calculated on the basis of empirical relation by PENZAR and PENZAR (1991):

$$Q'_s = Q_{so} [1 - (1-a)C] \tag{20}$$

where terms Q_{so} and a have the following meanings:

$Q_{so} \rightarrow$ global radiation for a bright sunny day on the fifteenth day of the month (GRBEC, 1989);

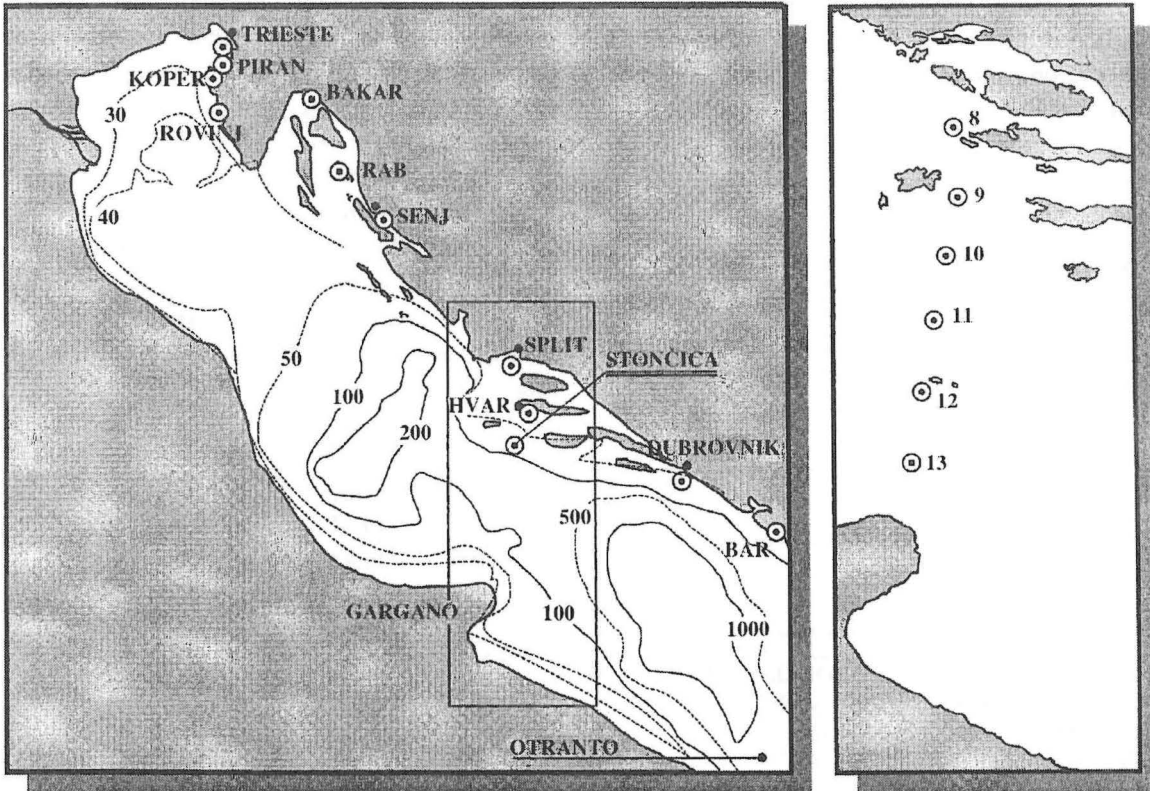


Fig. 1. Locations of meteorological and oceanographic stations along the eastern Adriatic coast. The box outlines the transect Split-Gargano in the middle Adriatic Sea

$a \rightarrow$ empirical constant with values 0.202 for April-October and 0.363 for November-March period.

The seasonal cycle of net heat flux (Fig.2) shows that from April to September the sea receives the heat from the atmosphere, reaching maximum in July (134.6 W m^{-2}). The sea loses most heat in December (112.1 W m^{-2}). At annual scale, the loss of heat is caused by long-wave radiation (60%), evaporation (33%), and much less with conduction (7%). The annual average for this particular station is $+7.9 \text{ W m}^{-2}$. Comparing these data with data found in literature (PICCO, 1991; SUPIĆ, 1993) it is evident that for different stations, although from the same geographic area, different heat fluxes were obtained. In the process of determination of individual components of thermal equilibrium, the selection of formula seems very important. Heat fluxes for the whole Mediterranean, GARRETT *et al.* (1993) showed differ-

ent results from those in this work. The discrepancies are related to selection of formulae used in calculation.

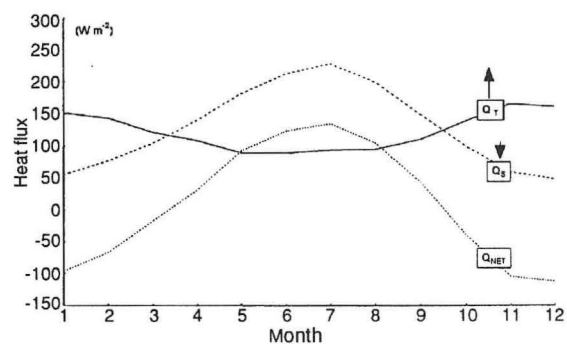


Fig. 2. Annual cycles of heat fluxes: solar radiation (Q_S), total outgoing (Q_T) radiation and net heat flux Q_{NET} . Total outgoing radiation is the sum of longwave, latent and sensible heat

The problem of evaporation over the Adriatic Sea was discussed elsewhere (GRBEC *et*

al., this issue). The SMITH (1980) formula was applied in this work. Mean seasonal cycles for the stations along the Adriatic coast are presented in Fig. 3.

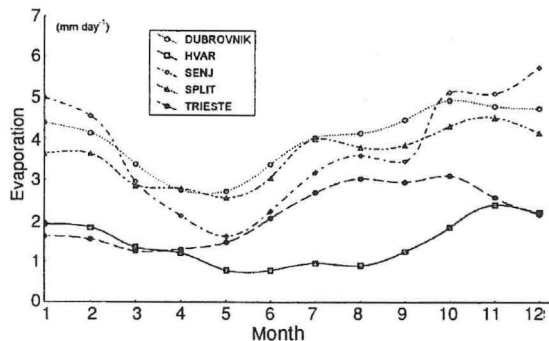


Fig. 3. Annual cycles of evaporation for stations along the eastern Adriatic coast

Table 3. Salinity and temperature dataset

STATION AT THE SPLIT-GARAGANO TRANSECT	PERIOD OF MEASUREMENTS	SOURCE
PELEGRIN P:08 (0,10,20,30,50,75 m)	1961-1980	INSTITUTE OF OCEANOGRAPHY AND FISHERIES - SPLIT
STONČICA P:09 (0,10,20,30,50,75,100 m)		
SUŠAC P:10 (0,10,20,30,50,75,100, 120 m)		
P:11 (0,10,20,30,50,75,100, 150, 170 m)		
PALAGRUŽA P:12 (0,10,20,30,50,75,100, 110 m)		
GARGANO P:13 (0,10,20,30,50,75,100, 110 m)		

Hydrographic and sea level dataset

The hydrographic dataset used in this work spans the time interval from January 1961 to December 1980. Data were collected on the regular monthly or seasonal cruises at oceanographic stations of the transect Split-Gargano

(see Fig. 1). Measurements were made mostly once a month (only exceptionally several time per month). Only the data with the same number of measurements for standard oceanographic depths (0, 10, 20, 30, 50, 75 and 100m) at stations 8,9,10,11,12 and 13 were used, while the data from the depths below 100m were rare, and were not considered (Table 3).

In addition to temperature and salinity, mean sea level data from permanent coastal stations (see Fig.1. and Table 4) were considered.

Table 4. Mean sea level dataset

MEAN SEA LEVEL		
STATION	PERIOD OF MEASUREMENT	SOURCE
TRIESTE	1988	ISTITUTO TALAS-SOGRAFICO - TRIESTE
KOPER ROVINJ BAKAR SPLIT DUBROVNIK BAR	1961-1980	NATIONAL HIDRO - METEOROLOGICAL OFFICE - ZAGREB

Sampling errors in the hydrographic dataset

Measurements of oceanographic variables are practically never continuous. Many of them have long measurement periods but include only few measurements. For example, temperature and salinity, at the open sea stations, were measured once per month. Therefore, "mean" monthly values represent only one value. With a finite number of samplings (mainly one), we must find an appropriate value in order to eliminate undersampling errors. Contrary to sea temperature and salinity, meteorological data were measured once an hour. Because the purpose of this work is to compare the conditions of sea and atmosphere, in order to have comparable time series, sampling errors of temperature and salinity must be determined. The

sampling errors were analyzed using the daily mean sea temperature from the coastal station Split in the period 1961-1980. At this station sea temperature was measured twice a day. The mean monthly sea temperature from daily measurements (T_{30}) at coastal station Split was compared to data obtained by measurements performed at the Split station on the same dates when sea temperatures were measured at the Stončica station (T_1). Maximum positive discrepancy between those monthly values ($T_{30} - T_1$) was $3.15\text{ }^{\circ}\text{C}$, while maximum negative discrepancy was $-2.80\text{ }^{\circ}\text{C}$. These considerable differences (Fig. 4) point to the fact that data should be filtered to ensure comparability of the data series at the annual scale. Moving average with $n=12$, applied to the dataset resulted with smaller differences between T_{30} and T_1 . Larger filtering window diminishes differences but reduces the data set (Fig.5) and the window $n=12$ seems to be an optimal choice for this dataset.

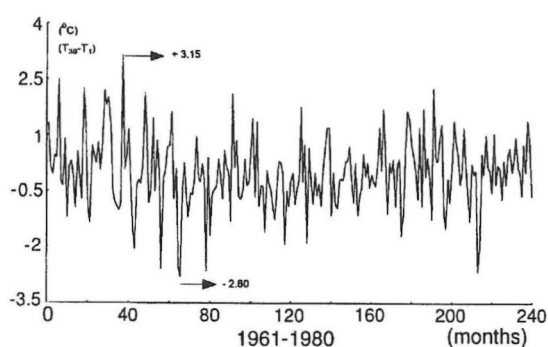


Fig. 4. The difference between mean monthly temperatures T_{30} and T_1 (coastal station Split)

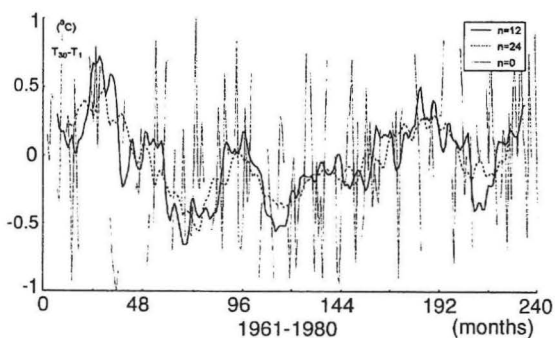


Fig. 5. Comparison of the difference ($T_{30} - T_1$) ($n=0$) to filtered differences with moving average of $n=12$ and $n=24$ window

Due to measurement circumstances at the sea, *in situ* oceanographic measurements are given an epithet of "nice weather oceanography". Indeed, when weather types are attributed to dates of measurements at Stončica station it is clear that most of measurements were done on anticyclonic weather conditions (A. BAJIĆ, personal communication).

RESULTS AND DISCUSSION

Secular variations

Basic climatic oscillations were determined for the meteorological time series with long oscillation periods. At the secular time scale, significant air pressure and sea level trends amounting to (1.01 ± 0.04) hPa/100 years and (14.4 ± 0.6) cm/100 years respectively, were obtained (Fig.6). Decreasing linear trend of precipitation with oscillation period of 57.7 years was found. Temperature changes at a secular scale were stationary with a climate

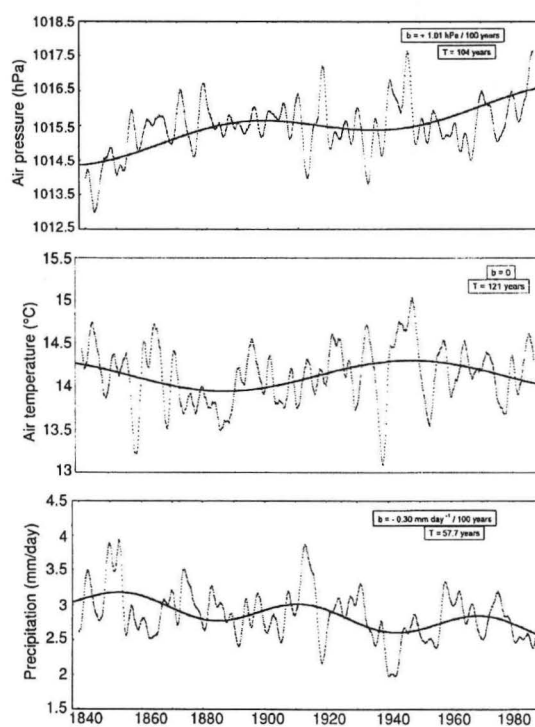


Fig. 6. Basic climatic oscillation of air pressure, air temperature and precipitation for Trieste station

wave of 121 years. Approximately the same length was found for pressure secular changes, while climatic oscillation for precipitation amounted to half of the mentioned period. The amount of these secular changes points to the fact that oceanographic parameters which depend on meteorological parameters could show the same secular changes as well.

Interannual variations

Interannual sea surface temperature and mean sea level variations

The time series of mean monthly anomaly of sea surface temperature (SST) and mean sea level (MSL) were subject to the principal component analysis in order to quantify the influence of possible climatic changes in the different regions in the Adriatic sea. For both time series, eigenvalues and factor matrix of the component loadings were determined (Tables 5 and 6) on the basis of significant correlation matrices. Applying the Rule N, only the first two components are significant for SST, while for MSL the first principal component describe sufficient variance (93.4%), having significant loading for all variables. Varimax rotation resulted in simple structure only in SST field, while components from MSL were left unrotated.

Table 5. Eigenvalues (λ) of the first two principal components and their contribution (%) to the total variance in sea surface temperature (SST) and mean sea level (MSL) field and eigenvalues of the random process (RP) for the matrix of the same size as original one

Principal component	SST		MSL		RP	
	λ_r	%	λ_r	%	λ_r	%
1	4.84	69.1	6.54	93.4		
2	1.12	16.0	0.25	3.6	0.85	12.2

PC analysis in the SST field separated two regions: the northern Adriatic on the one hand and the middle and the southern Adriatic on the other hand (note that the southern is represented only with the Dubrovnik station). According to spatial distribution of component

loadings in the northern Adriatic, station Rab differs from the other stations. The value of this component loading points to the fact that those processes which cause long term SST variability should have less impact on the Rab station. It can be explained by surface cooling, which, under the influence of bora, is weaker with the distance from the coast.

Table 5. Eigenvalues (λ) of the first two principal components and their contribution (%) to the total variance in sea surface temperature (SST) and mean sea level (MSL) field and eigenvalues of the random process (RP) for the matrix of the same size as original one

SST	COMPONENT	
STATION	PC ₁	PC ₂
TRIESTE	0.92	0.23
PIRAN	0.92	0.19
RAB	0.74	0.54
SENJ	0.84	0.30
SPLIT	0.49	0.80
HVAR	0.36	0.86
DUBROVNIK	0.09	0.87

MSL	COMPONENT	
STATION	PC ₁	PC ₂
TRIESTE	0.97	-0.17
KOPER	0.95	-0.21
ROVINJ	0.98	-0.04
BAKAR	0.95	-0.20
SPLIT	0.98	0.14
DUBROVNIK	0.97	0.21
BAR	0.96	0.27

Contrary to SST field, in the MSL field there are no spatial differences because interannual variation of MSL are similar throughout the Mediterranean basin (MAZZARELA and PALUMBO, 1989). The correlation matrix \mathbf{R} (not shown), as well as factor matrix of component loadings, display spatial homogeneity of the sea level. This means that throughout the Adriatic, hydrostatic pressure influences MSL with the same amount.

Temporal variation of SST and MSL fields were described with orthogonal PC scores. In order to explain possible atmospheric influ-

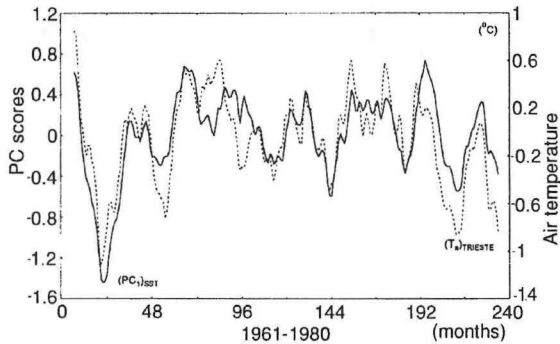


Fig. 7. Interannual variability of the first principal component from the SST field $(PC_1)_{SST}$ and air temperature for Trieste station $(T_a)_{TRIESTE}$

ences the PC scores were related to those processes that could cause variability. Since the starting manifest variables are mean monthly anomalies of the SST and MSL, correlation coefficients are calculated for anomaly series, and moving averages ($n=12$) are displayed in figures for clarity. In the SST field, the highest correlation coefficient is between the first PC and the air temperature for Trieste station (Fig.7). Going southward, the correlation coefficients between this component and the air temperature decreases while at the same time correlation coefficient between second PC and air temperature increase (Table 7) explaining stronger advection effect in the southern region than in the northern one. A significant part of MSL variations (PC_1) is explained by changes of atmospheric pressure over the Adriatic (Fig. 8) and the water flux at the air-sea interface (Table 8). A small amount of MSL interannual changes (PC_2) are in good relation to interannual SST variations. A considerable correlation coefficient amounting to 0.49 (significant at the 0.01 level) is found between the $(PC_1)_{SST}$ and $(PC_2)_{MSL}$. This points to the fact that in the northern Adriatic, MSL is affected by both pressure and temperature changes (Fig. 9).

Table 7. Correlation coefficients between first two principal components from the SST field and air temperature

r_{PC,AT^*}	$AT_{TRIESTE}$	AT_{HVAR}	$AT_{DUBROVNIK}$
PC_1	0.67	0.58	0.48
PC_2	0.20	0.44	0.33

* AT = air temperature

Table 8. Correlation coefficients between the first two principal components from the MSL field, air pressure (p) and water flux ($E-P$)

PC_1	r
$P_{TRIESTE}$	-0.84
$P_{DUBROVNIK}$	-0.71
$(E-P)_{TRIESTE}$	-0.34
$(E-P)_{DUBROVNIK}$	-0.51

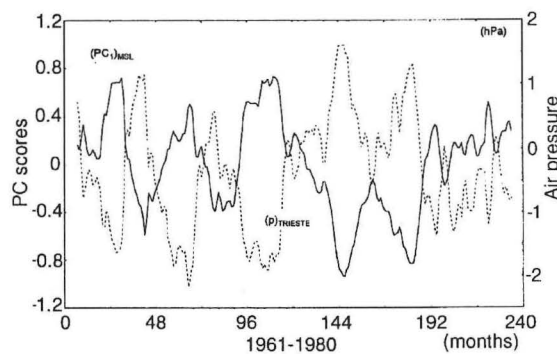


Fig. 8. Interannual variability of the first principal component from the MSL field $(PC_1)_{MSL}$ and air pressure for Trieste station $(p)_{TRIESTE}$

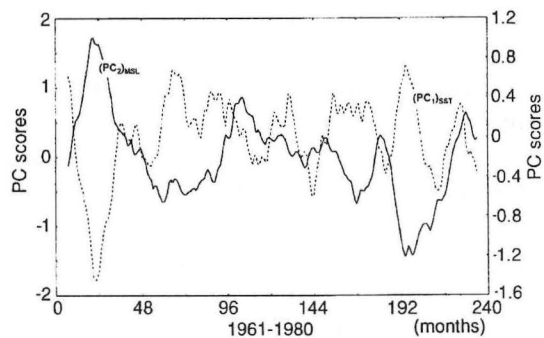


Fig. 9. Interannual variability of the first principal component from the SST field $(PC_1)_{SST}$ and second principal component from MSL field $(PC_2)_{MSL}$

Interannual temperature and salinity variations

In this subsection, the results of applying PCA to the seawater temperature (ST) and salinity (SAL) are presented in order to explain spatial and temporal variability. For this purpose, hydrographic parameters for station

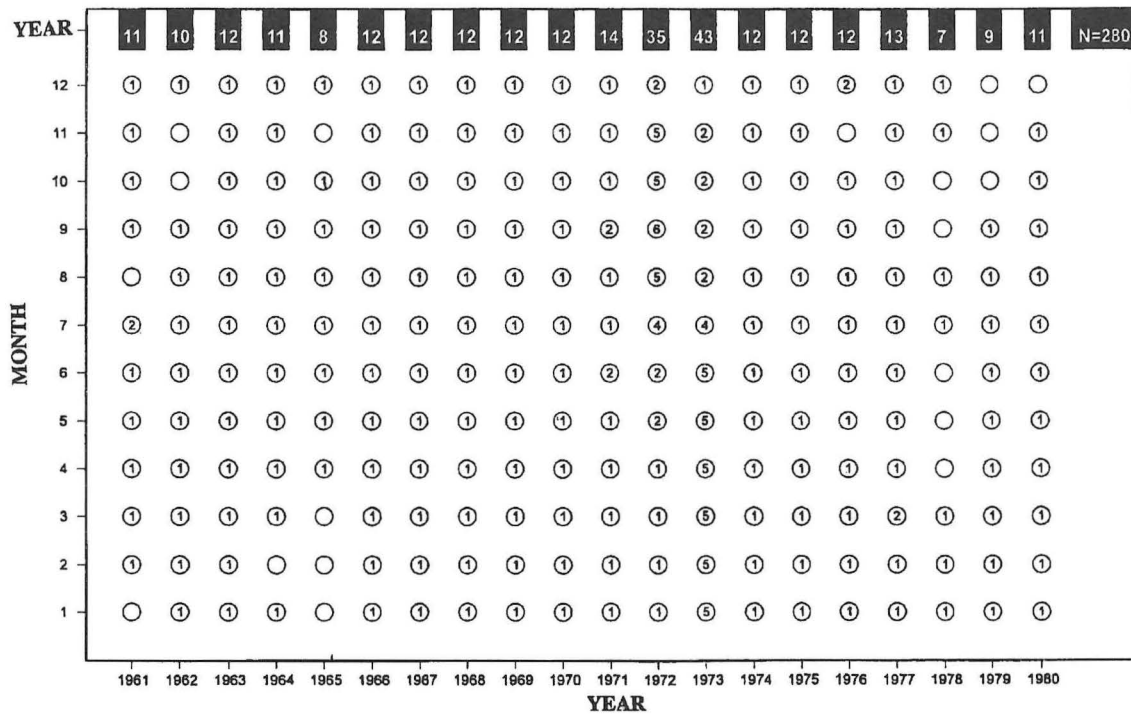


Fig. 10. Number of measurements per decade at Stončica station in the period 1961-1980

Stončica were used. Number of data are presented in Fig.10. For the reasons mentioned earlier in previous chapter, data were filtered before they were subject to principal component analysis. Eigenvalues (Table 9) and factor matrices of component loadings (Table 10) were determined for the first two principal components. Both for temperature and salinity, Varimax rotation was applied (Fig.11).

On the basis of distribution of PC loadings it was possible to distinguish two layers whose variability contributes with different amounts to the total variability in the temperature and salinity field. The first principal component has significant loadings for layer 30-100m. The second principal component has significant loadings in the surface layer down to 20m. PCA therefore recognizes two layers: the surface layer and the intermediate one. The corresponding component scores are presented in Fig.12. Temperature and salinity fluctuations in these two layers were explained comparing PC scores to atmospheric fluctuations. In the surface layer, significant correlation coefficient

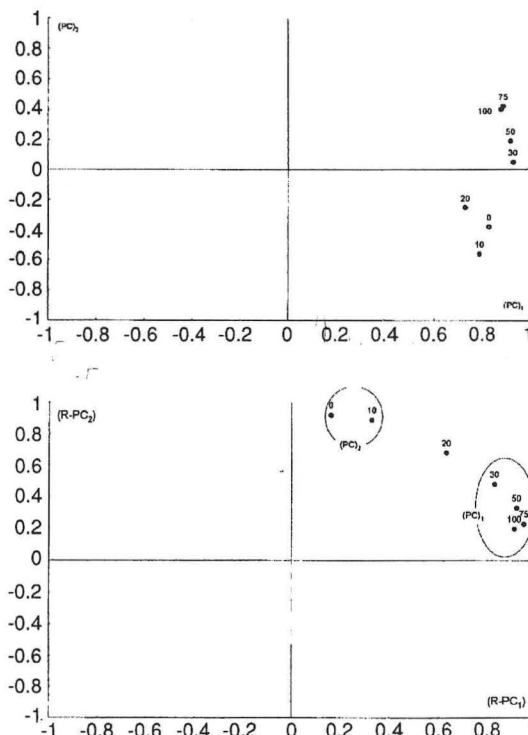


Fig. 11. Space representation (in coordinate frame of principal components) of factors matrix for the salinity field before (PC) and after Varimax rotation (R-PC)

Table 9. Eigenvalues (λ) of the first two principal components and their contribution (%) to the total variance in salinity (SAL) and sea temperature (ST) field and eigenvalues of the random process (RP) of the same size as the original one

Principal component	SAL		ST		RP	
	λ_r	%	λ_r	%	λ_r	%
1	6.01	87.2	5.40	77.2		
2	0.64	9.2	1.05	14.5	0.85	12.2

Table 10. Factor matrix of component loadings after Varimax rotation in salinity (SAL) and sea temperature fields (ST)

ST	COMPONENT	LOADINGS
DEPTH	PC ₁	PC ₂
S000	0.16	0.96
S10	0.21	0.97
S20	0.45	0.82
S30	0.75	0.59
S50	0.89	0.34
S75	0.95	0.22
S100	0.92	0.12

SAL	COMPONENT	LOADINGS
DEPTH	PC ₁	PC ₂
S00	0.16	0.92
S10	0.33	0.89
S20	0.63	0.68
S30	0.83	0.48
S50	0.92	0.33
S75	0.95	0.23
S100	0.91	0.20

(0.31) was found between PC₂ from the salinity field and E-P, with a three month lag. In the temperature field, significant correlation was found between the principal component for surface layer and net heat flux with 2 months lag.

In the intermediate layer salinity fluctuations (PC₁) are not affected by vertical processes and can be explained with horizontal advection of the saltier Mediterranean water. Higher salinity in the Mediterranean causes higher salinity in the middle Adriatic. As already known (ZORE-ARMANDA, 1972) the mechanism of exchange between the Adriatic

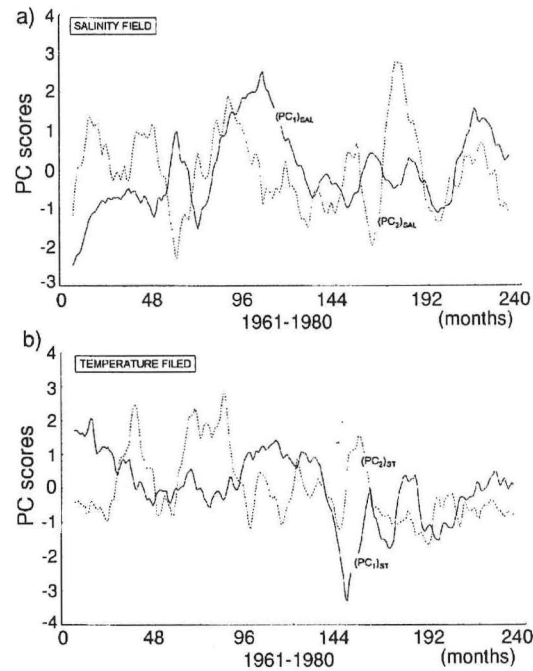


Fig. 12. Interannual variability of the first two principal components in the salinity a) and temperature field b)

and the Mediterranean can be explained by the horizontal pressure gradient between the northern and the southern Adriatic (pressure differences between Trieste and Palagruža). In the years with higher pressure differences, higher salinity in the intermediate layer of the middle Adriatic can be expected. A higher pressure gradient does not always correspond to higher salinity, due to various influences. Comparing the horizontal pressure gradient with salinity fluctuations in the intermediate layer (Fig.13) two characteristic periods are evident. In the period 1961-1970 salinity fluctuations are not accompanied by pressure gradient fluctuations. In this period their correlation was not significant because salinity in the Mediterranean was mainly increased due to the Assuan damm construction. It caused the fresh water input decrease from 41 to 11 km³ year⁻¹ (GERGES, 1976) which reflected upon higher salinity of the eastern Mediterranean. In the period 1973-1980, salinity fluctuations seem to respond to pressure gradient fluctuations and the correlation coefficient between them was 0.55 (significant at the 0.001 level).

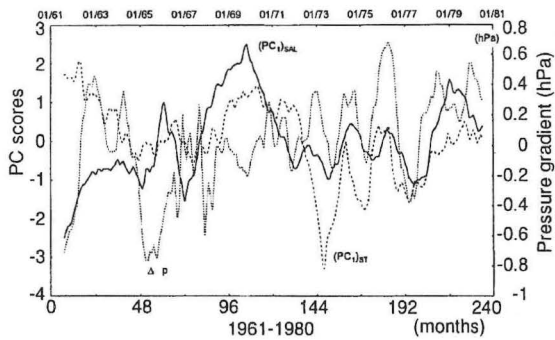


Fig. 13. Interannual variability of the first principal components for temperature $(PC_1)_{ST}$ and salinity $(PC_1)_{SAL}$ in the intermediate layer and air pressure gradient between Trieste and Palagruža

Besides by higher salinity, the LIW can be also detected in the intermediate layer of the middle Adriatic by higher temperature, so that the Mediterranean influence can also be seen through temperature. Like salinity fluctuations, the fluctuations of temperature also show two characteristic periods. In the second period, from 1973-1980 temperature fluctuations like the salinity ones, seem to reflect

ingressions. The correlation coefficient between temperature and pressure gradient in this period was 0.68 (significant at the 0.001 level).

At an interannual scale, it was possible to compare the salinity fluctuations with MSL fluctuations (Fig. 14). Both are the consequence of the water flux. Surface salinity and sea level changes are not directly related, but years of lower precipitation are characterized by higher salinity and higher density. At the same time lower precipitation causes lower sea level.

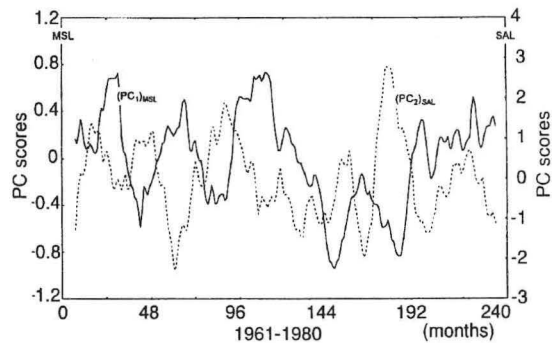


Fig. 14. Interannual variability of the second principal component for the salinity field $(PC_2)_{SAL}$ and first principal component for the MSL field $(PC_1)_{MSL}$

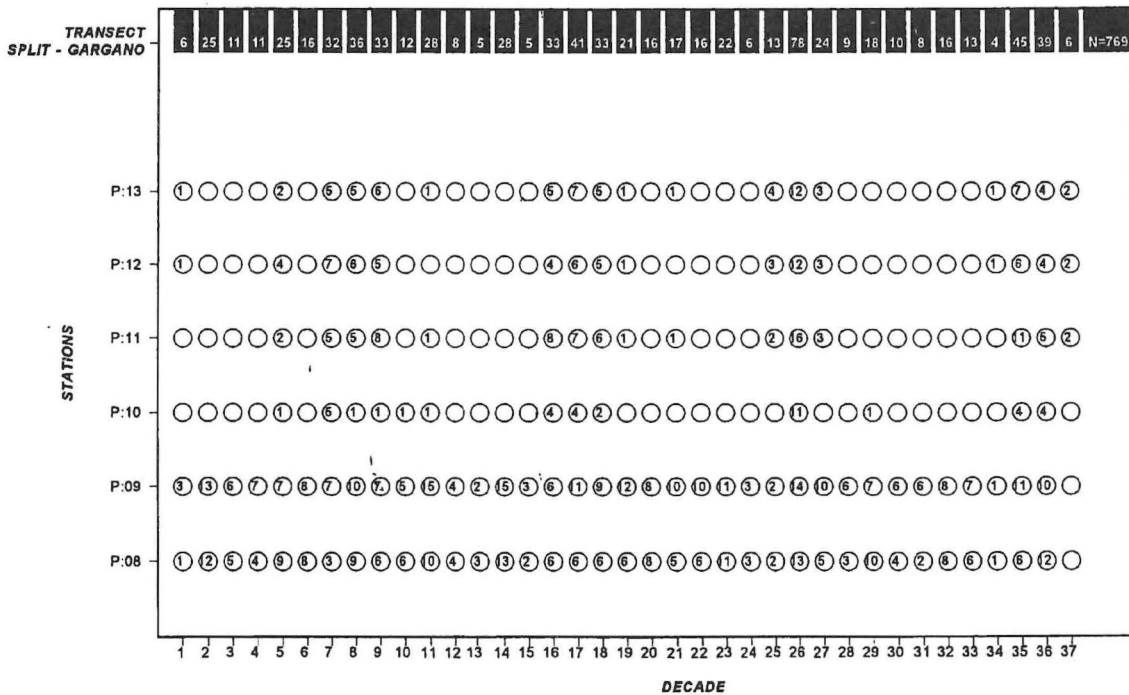


Fig. 15. Number of measurements per decade at the Split-Gargano transect for the period 1961 - 1980

Seasonal variations

Salinity and temperature data from the transect Split-Gargano were analyzed on an annual time scale, so that the data set extended from $t=1$ to $t=365$ days. Frequencies of data for every station, shown by ten-day periods are presented in Fig. 15.

In order to determine thermohaline fluctuations at the seasonal scale, temperature $T(x,z,t)$ and salinity $S(x,z,t)$ fields are determined where x represent station, z depth, and t sampling day of the year. These data matrices were used to determine seasonal cycles using the equation (18). Comparing the vertical temperature profile at stations 09 and 11 (Fig. 16), very small differences were found. So, the whole transect could be presented with a single seasonal cycle. The new data matrix was formed ($T(z,t)$ and $S(z,t)$) to represent the whole transect depending on the depth and the sampling date ($t=1, \dots, 365$). The mean annual cycle is determined by the harmonic analysis of temperature for all depths (Fig. 17). In the surface layer, 92% of the variance is explained by the equation (18), 91% and 78% at depths 10 and 20 m, respectively and from 72% to 37% at the depth from 30 to 100 m. Minimum and maximum temperatures occur with the phase lag relative to the heat flux from surface to the bottom. At the depth of 10 meters maximum temperature has a delay of 9 days in relation to the surface layer while at 20 meters maximum temperature has 48 days delay. The layers at 75 and 100 meters have a phase lag of 93 days relative to the surface. Minimum temperature in surface layer occurs in February, and at 75 and 100 meters at the beginning of March. The function of two harmonics shows the seasonal cycle of temperature at all depths showing isothermy in autumn and rather small temperature changes at 100 meters, which does not fall below 12 °C. Going to deeper layers, annual maximum occurs later in autumn while minimum at all depths occurs in the same month. This procedure seems to be sufficient for variables with a strong seasonal signal (like temperature and sea level) but it cannot be ade-

quate for other variables like salinity. This is confirmed when salinity data at seasonal scale are described with the function of two or more harmonics. Due to large standard deviation (Fig. 18) caused by large interannual salinity fluctuations, it is not possible to show seasonal salinity cycle with this analysis. Therefore the seasonal salinity cycle is determined by averaging within each month. The seasonal cycle (Fig. 19) shows salinity increase with depth. At the surface layer down to 10 meters there are two minima, in May and July. At the depth of 20 meters the secondary maximum disappears while the August maximum becomes more important.

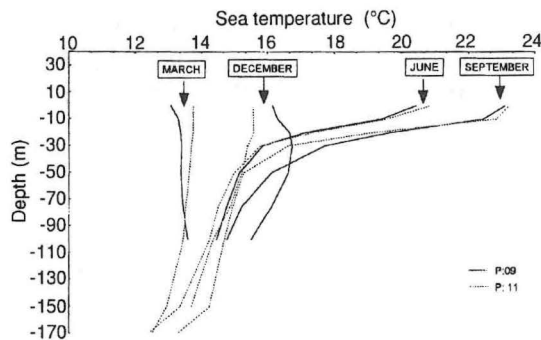


Fig. 16. Mean temperature profile for station 09 and 11 for different months

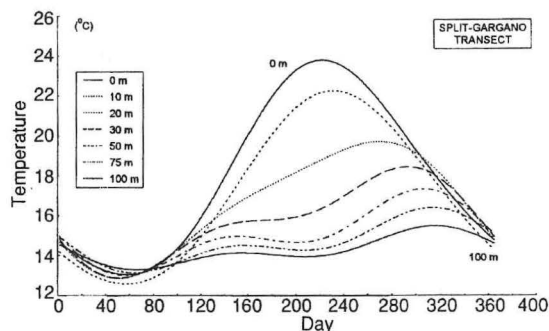


Fig. 17. Mean annual cycles of temperature and salinity at the standard oceanographic depths for the Split-Gargano transect

Large monthly salinity fluctuations are often reported in literature, but salinity is still conservative parameter at the monthly scale. Its large "monthly" fluctuations are due to large interannual fluctuations related to advection from the Mediterranean, while for exam-

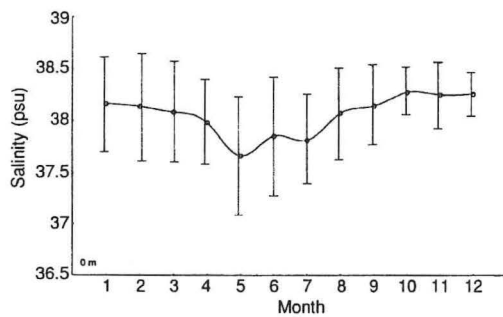


Fig. 18. Mean annual cycle of the surface salinity for the Split-Gargano transect. Vertical bars are standard deviations

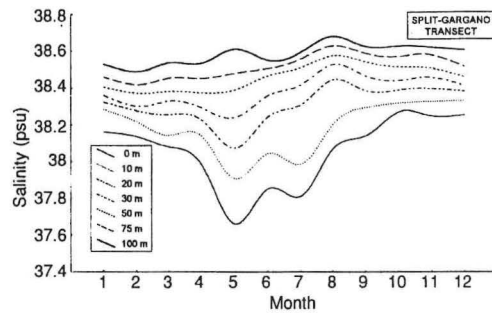


Fig. 19. Mean annual cycles of salinity at the standard oceanographic depths for the Split-Gargano transect. Mean annual cycles were determined averaging over the months

ple in the Gulf of California such fluctuations are caused by different long-term phenomena. The thermohaline fluctuations in the Gulf of California studied in a series of papers (BRAY, 1988; RIPA and MARINONE, 1989; CASTRO *et al.*, 1994) depend on phenomena like El-Niño, while the Adriatic is influenced by "ingression", which is the phenomenon of longer duration than El-Niño. So, monthly mean values obtained from data from the same month for all years had very large standard deviations.

Principal component analysis of temperature and salinity field

Standardised salinity and temperature values are represented with a set of data $Y_z(t)$ where t denotes an individual day and z the depth. Principal component analyses was performed on these matrices.

Table 11. Eigenvalues (λ) of the first three principal components and their contribution to the total variance (%) in salinity (SAL) and temperature fields (ST) and eigenvalue of the random process (RP) for the matrix of the same size as original one

Principal component	SAL		ST		RP	
	λ_r	%	λ_r	%	λ_r	%
1	5.09	72.7	4.89	69.9		
2	1.13	16.2	1.57	22.5		
3	0.32	4.6	0.28	4.0	0.81	11.5

The first three eigenvectors together describe 96.3 % of the temperature variance and 94.8% of the salinity variance (Table 11). Using three main components, the component loadings for temperature and salinity are determined and presented in Table 12. and Fig.20. The vertical distribution of temperature shows expected thermocline at the depth of 30-40 m (Fig.20a), while the one related to salinity shows halocline at almost the same depth (Fig.20b). Standardised values of the PC scores

Table 12. Factor matrix of component loadings after Varimax rotation in salinity and temperature fields

SAL	COMPONENT			LOADINGS
	PC ₁	PC ₂	PC ₃	
DEPTH				
S00	0.16	0.96	0.13	
S10	0.22	0.78	0.50	
S20	0.41	0.49	0.72	
S30	0.65	0.31	0.65	
S50	0.74	0.23	0.55	
S75	0.89	0.16	0.37	
S100	0.98	0.20	0.14	

ST	COMPONENT			LOADINGS
	PC ₁	PC ₂	PC ₃	
DEPTH				
S00	0.13	0.98	0.10	
S10	0.15	0.97	0.15	
S20	0.29	0.78	0.49	
S30	0.56	0.54	0.60	
S50	0.76	0.27	0.55	
S75	0.91	0.16	0.32	
S100	0.98	0.13	0.02	

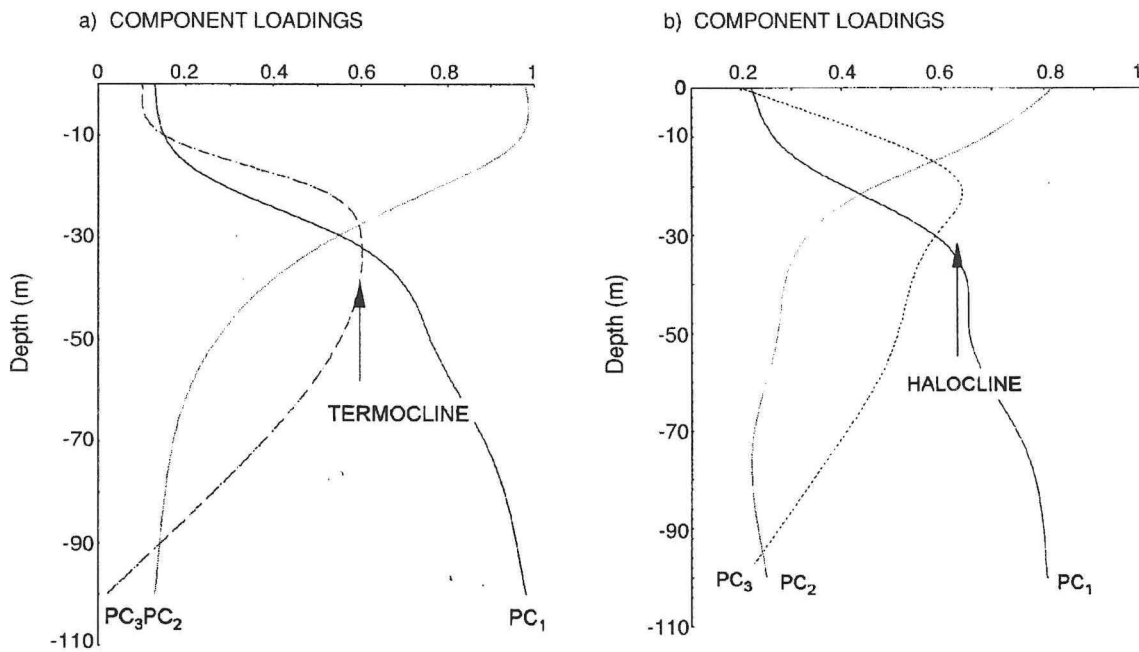


Fig. 20. Vertical structure of the first three principal components loadings in temperature a) and salinity b) field

are, because of the time scale, related to particular days. In order to present PC scores for each day of the year, harmonic function (equation 18) was fitted to the data, taking into account the fact that $A_0 = 0$. It is necessary to note that orthogonality of the main components is lost through this process. This analysis was possible only for temperature. The harmonic functions, which were fitted to the component scores, explain 93% of the variance of PC_2 (significant at the 99% level), 38% of the PC_1 and 30% of PC_3 , both significant at the 95% level.

In the surface layer, discrepancies of the component scores and the interpolated seasonal values of temperature, except for few values only, were not considerable. The largest discrepancies in the surface layer occurred in July and August. The largest positive discrepancies were found in the summer time and at the beginning of the cold season (Fig. 21a). In the deeper layers considerable discrepancies were found in autumn in November (PC_1) (Fig. 21b) and in October (PC_3) (not shown). The maximum discrepancies were delayed in deeper layers, relative to the surface.

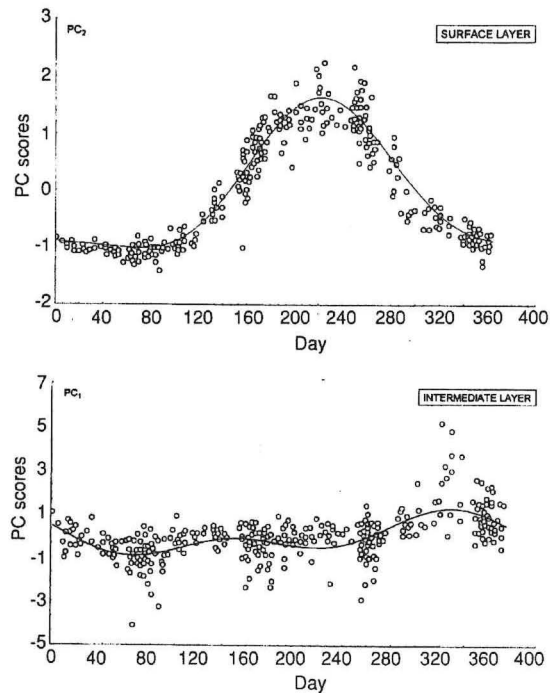


Fig. 21. Individual PC scores for temperature (circles) and interpolated seasonal curve (solid line) for the surface a) and intermediate b) layer

It was not possible to obtain the statistically significant fit for the PCs in the salinity field. Interpolated seasonal course, equation (18), describes less than 25 % of the variance pointing to the large interannual salinity fluctuations (ZORE-ARMANDA *et al.*, 1991). The corresponding PC scores, shown in Fig. 22, were determined by averaging over the months, and are presented using the cubic spline function (FRITSCH, 1971).

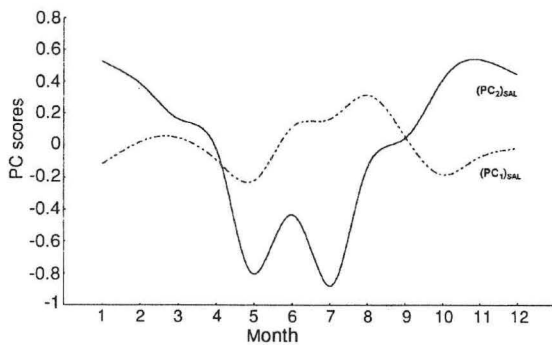


Fig. 22. Mean annual cycles of the PC scores for the surface $(PC_2)_{SAL}$ and intermediate $(PC_1)_{SAL}$ layers in the salinity field shown as cubic spline interpolation of monthly mean values

In the temperature field, component scores which correspond to the surface layer (PC_2) were correlated with the heat flux for the Hvar station (correlation coefficient was $r=0.82$ for the time lag of 31 days). Function (18) was fitted to the heat flux data and the obtained values were compared to the component scores of the PCA.

Component scores of PC_1 , which correspond to the deeper layers, lag four months behind the heat flux. Component scores had two maximum values: in May and in November (Fig.23). Maximum values in May are the consequence of the fast transport of heat in deep layers as the thermocline layer is not yet formed to prevent the vertical mixing process. In summer, when thermocline is formed, deeper layers do not receive heat, and lower temperatures are present. The temperature drop below the thermocline, when the thermocline is fully developed, is attributed to upwelling. Lower temperatures are observed below the

thermocline layer throughout the summer (ZORE-ARMANDA, 1969a). Besides the heat flux, the influence of wind on temperature of the water column is also considerable (Fig.24). Increase of wind speed in autumn corresponds to an increase in temperature of deeper layers. The heat from the warm surface layers is transported to the deeper layers by wind induced mixing.

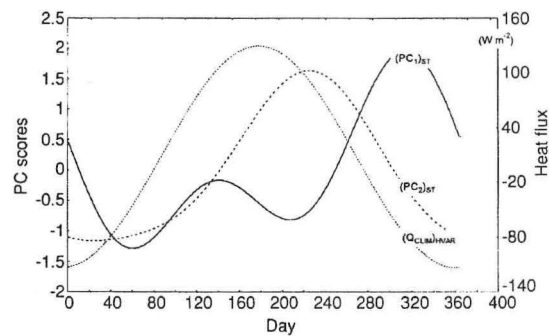


Fig. 23. Mean annual cycles of the $(PC_1)_{ST}$ and $(PC_2)_{ST}$ scores in the temperature field and net heat flux at the air-sea interface

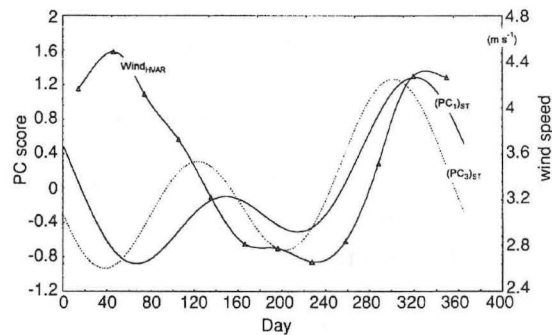


Fig. 24. Mean annual cycles of the $(PC_1)_{ST}$ and $(PC_3)_{ST}$ scores in the temperature field and wind speed at Hvar station

In the salinity field, component scores corresponding to the surface layer (PC_2) during the heating season are proportional to P-E differences, while in autumn and winter PC_2 scores and P-E differences are opposed in phase (Fig.25). Earlier investigations (PUCHER-PETKOVIĆ and ZORE-ARMANDA, 1973) proved that north Italian rivers, especially the Po River, influenced waters of the Jabuka Pit. When the thermocline is well developed, lighter

north Italian waters reside in the surface layer and are transported by the SE current to the Split-Gargano transect (ZORE-ARMANDA, 1956). They bring about a decrease of salinity in the surface layer. As a consequence of ice melting, the largest Po runoff is observed in May coinciding with salinity spring minimum at the transect (Fig.26). In summer, due to current system in the intermediate layer (ZORE-ARMANDA, 1969b), advection of saltier water from the southern Adriatic (Mediterranean) is observed. Less saline water resides at the surface, since the mixing is prevented by the fully developed thermocline, and in the summer period in the middle Adriatic the influence of the Po River inflow could be observed. In addition to seasonal forcing, component scores which correspond to salinity, are also controlled by specific dynamic conditions at the Palagruža Sill.

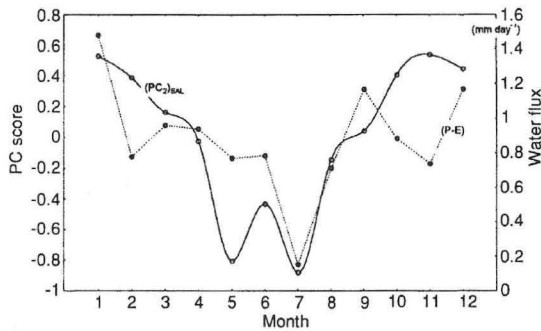


Fig. 25. Mean annual cycle of the $(PC2)_{SAL}$ scores for salinity (surface layer) compared to the difference between precipitation and evaporation (P-E)

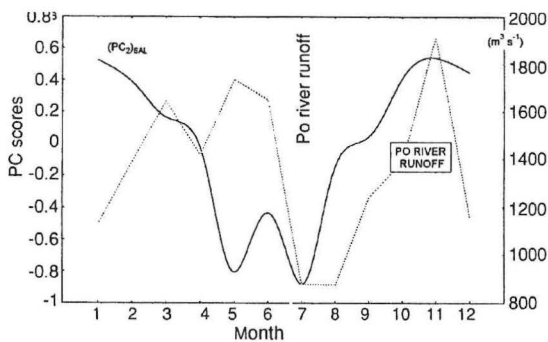


Fig. 26. Mean annual cycle of the PC_2 scores for salinity (surface layer) compared to the Po River runoff (in $10^3 m^3 s^{-1}$; mean values for the period 1961-1970; *Annali Idrologici*)

It is evident that vertical mixing processes have essential role on thermohaline properties of the whole water column. These vertical processes are under direct atmospheric influence. In addition, thermohaline properties are also under considerable influence of horizontal advection process, which depends both on oceanographic and meteorological conditions.

Seasonal heat and salt exchange

The results of PCA helped to resolve three characteristic layers: 0-20, 20-50 and 50-100 m. For these layers, temperature and salinity mean values were determined (Fig.27) by vertical integration between the top and the bottom of each layer. The integral was approximated using the trapezoidal rule. Vertical eddy diffusion coefficients in the surface layer were determined using turbulence formulae:

$$Q = K_H \rho_w c_{pw} \left. \frac{\partial T}{\partial z} \right|_{z=0}, \quad (21)$$

$$E-P = \frac{K_s}{\langle S \rangle} \left. \frac{\partial S}{\partial z} \right|_{z=0}.$$

Surface boundary conditions were applied with climatological values for heat and water fluxes Q_{CLIM} and $(E-P)_{CLIM}$ calculated for the Hvar station.

Vertical gradients of temperature and salinity were determined from the difference between the surface and 10 meters depth. Correlation coefficient between the vertical heat gradient and the heat flux is 0.91 (significant at the 99% level). It allowed us to determine vertical eddy diffusion coefficient for heat using the least square method. Mean annual cycles of vertical eddy diffusion coefficient is shown in Fig.28. The value obtained by the least squares method (Fig.29) is:

$$K_H = (3.05 \pm 0.09) \cdot 10^{-4} m^2 s^{-1}. \quad (22)$$

The net heat flux obtained by climatological values of bulk variables and the one obtained by turbulence formula are presented in Fig.30.

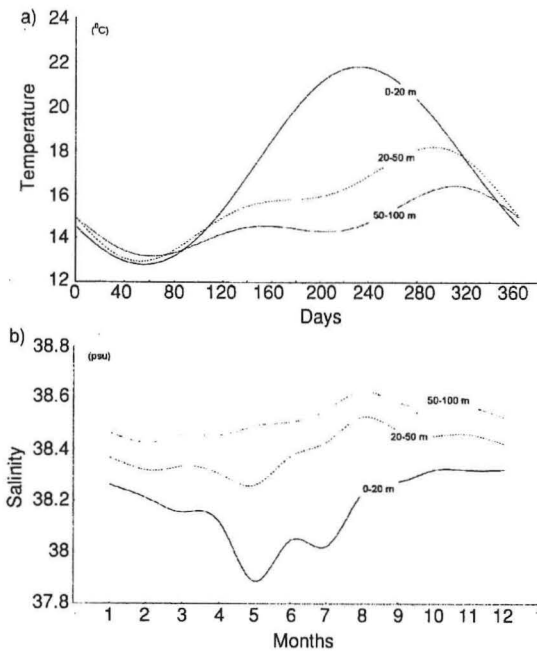


Fig. 27. Mean annual cycles of the mean sea temperature a) and salinity b) for the selected layers at the Split-Gargano transect

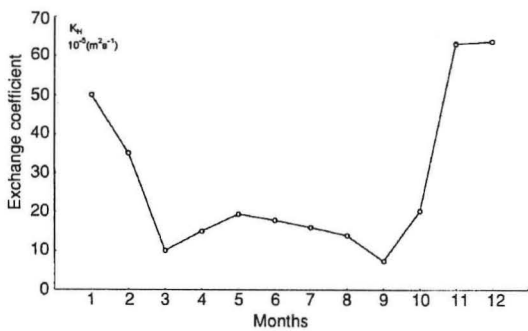


Fig. 28. Mean annual cycle of vertical eddy diffusion coefficient for the surface layer obtained using vertical temperature gradient

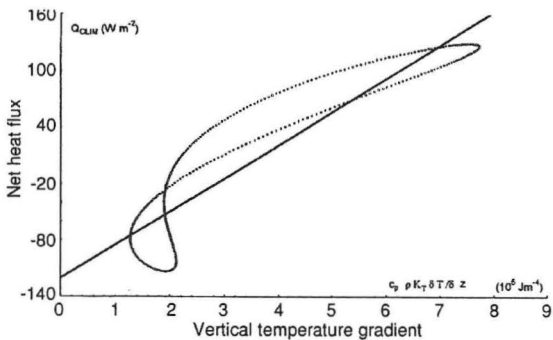


Fig. 29. Regression plot of net heat flux (Q_{CLIM}) and vertical temperature gradient at the surface. The slope of the regression line (bold) gives the best estimate of the vertical eddy diffusion coefficient

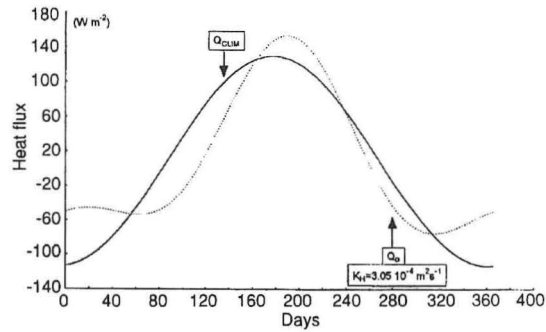


Fig. 30. Mean annual cycles of net heat flux calculated with climatological means of bulk variables (solid curve) and estimated by the turbulence formula with $K_H = 3.05 \cdot 10^{-4} \text{ m}^2 \text{ s}^{-1}$

The relationship between the water flux and surface salinity has already been discussed. Vertical eddy diffusion coefficient for the surface layer is determined again, using different relations for the water flux trough the year, as indicated in the schema:

$$E-P = \begin{cases} (E-P) & \text{September - April} \\ E-(P+R_{PO}) & \text{May - August} \end{cases} \quad (23)$$

were R_{PO} denotes the quotient between the Po River inflow and the area of the Adriatic shelf. Taking the Po runoff into account, correlation coefficient between water flux and vertical salinity gradient in the surface layer was 0.83, (significant at the 99% level) (Fig.31), enabling determination of the vertical eddy diffusion coefficient (Fig. 32). The value obtained by the least squares method (Fig. 33) is:

$$K_S = (0.406 \pm 0.09) \cdot 10^{-4} \text{ m}^2 \text{ s}^{-1}. \quad (24)$$

This value is an order of magnitude lower than the eddy diffusion coefficient obtained using turbulence formulae for heat flux. Using the value $K_S=0.406 \cdot 10^{-4} \text{ m}^2 \text{ s}^{-1}$, water flux (E-P) was determined and compared with the one estimated by climatological mean values (Fig.34). The value of K_H is well within the typical oceanic range (RIPA and MARINONE, 1989) and to that one calculated for the northern Adriatic (MALAČIĆ, 1991; SUPIĆ, 1993). In earlier investigations in the middle Adriatic, vertical eddy diffusion coefficient was not cal-

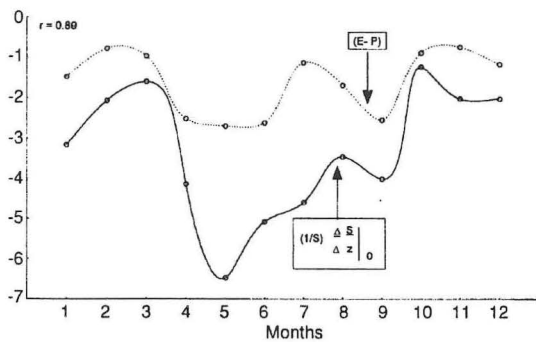


Fig. 31. Mean annual cycles of climatological water flux $(E-P)_{CLIM}$ and vertical salinity gradient at the surface. Climatological water flux was calculated using parametrisation (23)

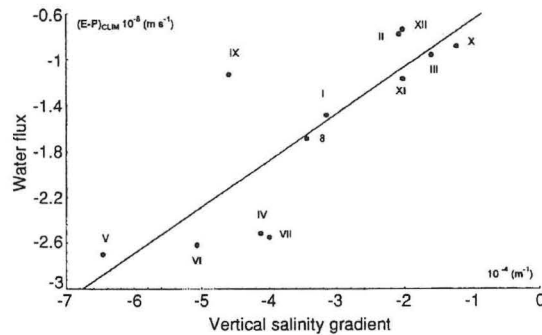


Fig. 33. Regression plot of the water flux $(E-P)_{CLIM}$ and vertical salinity gradient at the surface. The slope of the regression line (bold) gives the best estimate of the vertical eddy diffusion coefficient

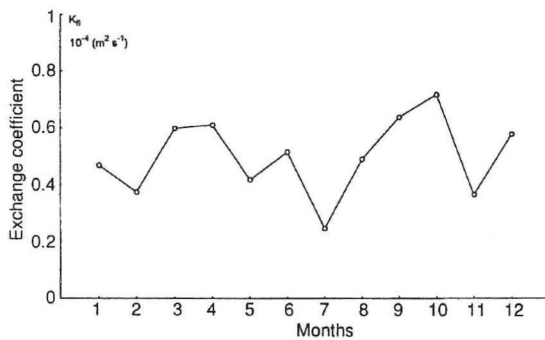


Fig. 32. Mean annual cycle of eddy diffusion coefficient for the surface layer obtained using vertical salinity gradient

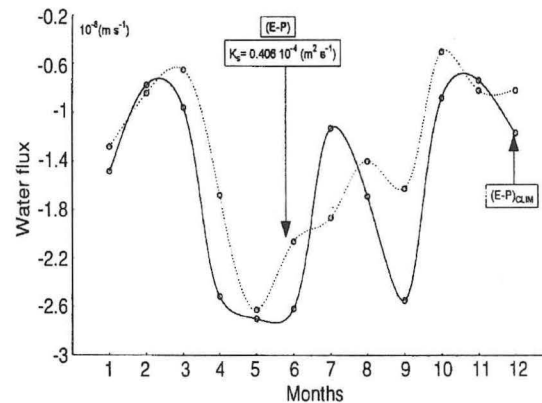


Fig. 34. Mean annual cycles of the water flux calculated using parametrisation (23) and estimated by the turbulence formula with $K_S = 0.406 \cdot 10^{-4} \text{ m}^2 \text{ s}^{-1}$

culated for the whole year on the basis of the long-term data set. For summer season ZORE-ARMANDA (1963) has obtained a somewhat larger value.

Finally, it was possible to determine vertical contribution to heat and salt in particular layers of the water column and to compare it with the rate of change of heat and salt content which was determined using equations (15-17) and Stirling's formula of centered finite differences (SCHEID, 1968).

The results for the upper layer are presented in Fig.35. Thermohaline changes in that layer are the consequence of vertical processes, being under the atmospheric influence throughout the year. However, in summer season ther-

mohaline changes are also under the horizontal advective control. From March to May heat content changes, following the changes that originate from vertical processes. In this period there is no heat transport from either the southern or northern Adriatic, according to well known circulation patterns. After development of the thermocline, the two curves separate. The cooling of the surface layer is weaker than that due to vertical heat content change. The difference is attributed to the horizontal advection of water from the northern Adriatic. This water is warmer in the summer season than the water of the middle Adriatic. This horizontal contribution to the heat content change in upper 20m in the summer is observed in salt content

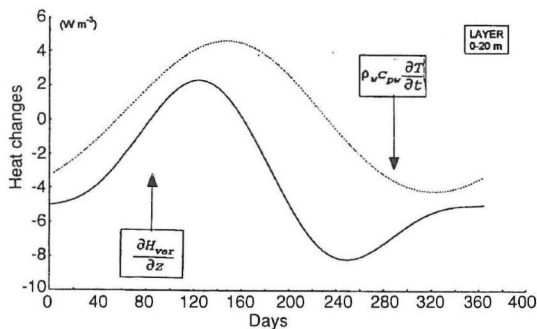


Fig. 35. Rate of change of the heat content in the upper 20 m (dotted line) and difference in the vertical fluxes at the top and bottom of the layer (solid line)

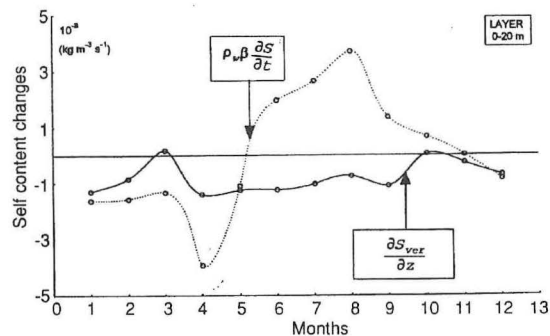


Fig. 36. Rate of change of the salt content in the upper 20 m (dotted line) and difference in the vertical fluxes at the top and bottom of the layer (solid line)

change as well, since the water from the northern Adriatic is less saline. It causes large salinity changes and minimum salinity values in the surface layer in the summer time.

In the middle layer, between 20 and 50 m (Fig. 36), it is more difficult to explain the relationship between vertical and horizontal contribution to the heat and salt rate change, especially in the season of the fully developed thermocline. The differences are partly due to the value of the vertical eddy diffusion coefficient. In this layer, significant difference is observed between salt content change due to vertical processes and the total salt content change. This difference accounts for the salinity increase due to advection of saltier southern Adriatic or Mediterranean waters.

While in the surface layer (the above thermocline) processes are under the direct atmospheric influence, in the deeper layer are considerably influenced by horizontal processes which are also the consequences of atmospheric influence.

CONCLUSIONS

At the secular time scale significant increase trends were observed for air pressure and sea level and the decrease trends were observed for precipitation. Secular changes of air temperature are well described by the basic

climatic wave with a 121 year period. The pressure increase trend shows the same basic oscillation (104.1 years) while precipitation has 57.7 years period. The sea level trend is a part of a very long period (1170 years) which at the secular scale can be considered linear. So, secular changes point to the possibility that associated oceanographic parameters could have secular changes as well. The sea level changes in the same way all along the Adriatic, while the changes of sea temperature are very small and significant only in the northern Adriatic. The sea level increase at the secular scale cannot be related to the decrease of precipitation and the increase of air pressure over the Adriatic. This means that secular changes of the sea level are the consequence of global changes.

The sea surface temperature is the consequence of atmospheric heating influenced by local disturbances from wind and surface cooling which is stronger in the northern than in the middle and southern Adriatic. As there is no significant temperature increase at the secular scale, surface temperature increase could not be expected. However, in the surface layer seasonal cooling caused by the wind and evaporation in the northern Adriatic is stronger than in the middle and southern Adriatic. With stronger influence of air temperature on sea temperature possible secular changes in the atmosphere are easier to observe here than in

other Adriatic areas. In deeper layers temperature changes are the consequence of horizontal advection. Due to advection increase, temperature increase could be expected in the intermediate layer of the Adriatic.

From the analysis of salinity field it can be concluded that PCA was successfully applied to these data, separating only two layers whose salinity properties change due to different processes. In the surface layer salinity change occurs due to water flux influence. In the intermediate layer salinity is under considerable influence of horizontal advection. Salinity change in the intermediate layer is highly correlated to horizontal pressure gradient between the northern and southern Adriatic. Therefore, at a secular scale, salinity increase in the intermediate layer is a consequence of horizontal pressure gradient increase.

Thermohaline processes are under the influence of vertical and horizontal processes. In the surface layer in summer thermohaline properties change with vertical and horizontal processes with advection of warmer and less salty northern Adriatic water. Horizontal pro-

cesses are considerable only during the presence of the thermocline when fresh water remains in the surface layer and, brought by currents, reaches the Palagruža sill. In other seasons thermohaline is under the influence of vertical processes. Deeper layers are characterized by the advection from the southern Adriatic or Mediterranean during summer while in other seasons vertical processes predominate.

ACKNOWLEDGMENTS

Author gratefully acknowledges Mira ZORE-ARMANDA for discussion of coastal and open sea dynamic and water mass formation. Author wishes to thank Mirko ORLIĆ for helpful suggestions and comments. Thanks are also to Miroslav GAČIĆ for his constructive remarks and to Krešo PANDŽIĆ for his comments of principal component analysis. This work was supported by Ministry of Science of the Republic of Croatia and by Intergovernmental Oceanographic Commission under the contract SC-2141277.

REFERENCES:

- ANNALI IDROLOGICI. Parte II 1961-1970. Ministero dei Lavori Pubblici, Roma.
- BRAY, N.A. 1988. Thermocline circulation in the Gulf of California. *J.Geophys.Res.*, 93: 4993-5020.
- BULJAN, M. 1953. Fluctuations of salinity in the Adriatic. *Izvješća-Rep. Exp. Hvar*, 2(2): 1-64.
- BULJAN, M. 1964. An estimate of productivity of the Adriatic Sea made on the basis of its hydrographic properties. *Acta Adriat.*, 11(4): 35-45.
- BULJAN, M. 1974. Basic characteristics of the Adriatic Sea as a production basin. *Acta Adriat.*, 16(2): 31-62.
- BULJAN, M. and M. ZORE-ARMANDA. 1976. Oceanographic properties of the Adriatic Sea. *Oceanogr. Mar. Biol. Ann. Rev.*, 14: 11-98.
- BULJAN, M. and M. ZORE-ARMANDA. 1979. Hydrographic properties of the Adriatic Sea in the period from 1971 through 1983. *Acta Adriat.*, 20: 1-368.
- CASTRO, R., M.F. LAVIN and P. RIPA. 1994. Seasonal heat balance in the Gulf of California. *J.Geophys.Res.*, 99: 3249-3261.
- FRITSCH, J.M. 1971. Objective analysis of a two-dimensional data field by the cubic spline technique. *Month. Weath. Rev.*, 99: 379-385.
- FULGOSI, A. 1988. Factor analysis. *školska Knjiga*, Zagreb, 367 pp.
- GARRETT, C., OUTERBRIDGE, R. and THOMPSON, K. 1993. Interannual variability in the Mediterranean heat and buoyancy fluxes. *J. Climate*, 6: 900-910.
- GERGES, M.A. 1976. The damming of the Nile river and its effect on the hydrographic condition and circulation pattern on south-eastern Mediterranean and Sues Channel. *Acta Adriat.*, 18: 179-191.
- GILL, A.E. 1982. *Atmosphere-Ocean Dynamics*. Academic Press. Orlando, 662 pp.
- GRBEC, B. 1989. Determining the persistence of solar irradiation with first step Markov chains. M.Sc. thesis (in Croatian). University of Zagreb, 95 pp. (mimeo)
- GRBEC, B. and V. KOVAČEVIĆ. 1995. Temperature measurements at two sea surface levels in Trieste harbour in 1988. *Boll.Ocean.Teor. Appl.*, 11:103-111.
- MALAČIĆ, V. 1991. Estimation of vertical eddy diffusion coefficient on heat in the Gulf of Trieste (Northern Adriatic). *Oceanologica Acta*, 14: 23-32.
- MAZZARELA, A. and A. PALUMBO. 1989. Recent changes of mean sea level in the Mediterranean area. *Boll. Ocean. Teor. Appl.*, 7: 285-292.
- MORCOS, S. 1972. Sources of the Mediterranean intermediate water in the Levantine Sea. In: A.L. Gordon (Editor). *Studies in physical oceanography*. Gordon & Breach Science Publishers. New York. N.Y., pp. 185-206.
- ORLIĆ, M., M. GAČIĆ and P. LAVIOLETTE. 1992. The current and circulation of the Adriatic Sea. *Oceanologica Acta*, 15: 109-124.
- OVERLAND, J.E. and R.W. PREISENDORFER. 1982. A significance test for principal component applied to a cyclone climatology. *Mon. Weath. Rev.*, 101: 1-4.
- PREISENDORFER, R.W. 1982. *Principal component analysis in meteorology and oceanography*. Elsevier. Amsterdam, 425 pp.
- PENZAR, I. and B. PENZAR. 1991. Hourly values of solar irradiation in clear skies. *Geofizika*, 8: 33-42.
- PICCO, P. 1991. Evaporation and heat exchanges between the sea and the atmosphere in the Gulf of Trieste during 1988. *Il Nuovo Cimento*, 14 C: 335-345.
- PUCHER-PETKOVIĆ, T. and M. ZORE-ARMANDA. 1973. Essai d'évaluation et pronostic de la production en fonction des facteurs du milieu dans l'Adriatique. *Acta Adriat.*, 15(1): 1-37.
- RICHMAN, R.W. 1986. Rotation of principal components. *J. Climatol.*, 3: 293-335.
- RIPA, P. and S.G. MARINONE. 1989. Seasonal variability of temperature, salinity, velocity and sea level in the central Gulf of California as inferred from historical data. *Q.J.R.Met.Soc.*, 115: 887-913.

- SCHEID, F. 1968. Theory and problems of numerical analysis. Shaum's outline series. Mc Graw-Hill. New York, N.Y., 422 pp.
- SMITH, S.D. 1980. Wind stress and heat flux over the ocean in gale force winds. *J. Phys. Oceanogr.*, 10:709-726.
- SPIEGEL, F. 1972. Probability and statistics. Shaum's outline series. Mc Graw-Hill. New York, N.Y., 321 pp.
- SUPIĆ, N. 1993. Surface fluxes and hydrographic characteristics of the Northern Adriatic. M.Sc. thesis (in Croatian), University of Zagreb, 124pp. (mimeo)
- THOMPSON, R.O.R.Y. 1983. Low pass filters to suppress inertial and tidal frequencies. *J. Phys. Oceanogr.*, 13:1077-1083.
- TZIPERMAN, E. and P. MALANOTTE-RIZOLI. 1991. The climatological seasonal circulation of the Mediterranean Sea. *J. Mar. Res.*, 49: 411-434.
- ZORE-ARMANDA, M. 1956. On gradient currents in the Adriatic Sea. *Acta Adriat.*, 6: 1-38.
- ZORE-ARMANDA, M. 1963. Les masses d'eau de la mer Adriatique. *Acta Adriat.*, 10(3): 1-94.
- ZORE-ARMANDA, 1969a. Temperature relations in the Adriatic Sea. *Acta Adriat.*, 13(5): 1-50.
- ZORE-ARMANDA, M. 1969b. Water exchange between the Adriatic and the Eastern Mediterranean. *Deep-Sea Res.*, 16: 171-178.
- ZORE-ARMANDA, M. 1969c. Origine possible des fluctuations de la salinité de l'eau de la mer Adriatique. *Rapp. Comm. int. Mer Medit.*, 19(4): 719-722.
- ZORE-ARMANDA, M. 1972. Response of the Mediterranean to the oceanographic /meteorological conditions of the Northern Atlantic. *Rapp. Comm. int. Mer Medit.*, 21(4): 203-205.
- ZORE-ARMANDA, M. 1974. Formation of eastern Mediterranean deep water in the Adriatic. *Coll. Internat. C.N.R.S.*, 215: 127-133.
- Zore-Armanda, M. 1991. Natural characteristics and climatic changes of the Adriatic Sea. *Acta Adriat.*, 32(2): 567-586.
- ZORE-ARMANDA, M. and M. BONE. 1987. The effect of bottom topography on the current system of the open Adriatic sea. *Boll. Oceanol. Teor. Appl.* 5: 3-18.
- ZORE-ARMANDA, M., M. BONE, V. DADIĆ, M. MOROVIĆ, D. RATKOVIĆ, L. STOJANOSKI and I. VUKADIN. 1991. Hydrographic properties of the Adriatic Sea in the period from 1971 through 1983. *Acta Adriat.*, 31:5-547.

Accepted: 29 September 1997.

Appendix

σ	→ Stefan-Boltzman's constant: $5.67 \cdot 10^{-8}$ ($\text{W m}^{-2} \text{K}^{-4}$),	K_S	→vertical eddy diffusion coefficient of salt: ($\text{m}^2 \text{s}^{-1}$)
ρ_w	→ water density: 1024 (kg m^{-3}),	L	→latent heat of sea water: $2.5 \cdot 10^6$ (J kg^{-1}),
ρ_a	→ air density: 1.25 (kg m^{-3}),	n	→number of data
α	→ albedo of sea surface	N	→number of variables
β	→ compressibility of sea water: $7.2 \cdot 10^{-4}$ (psu)	PC_r	→r's principal component
λ_i	→eigenvalues	P_r	→contribution of first r principal components (%)
$\langle s \rangle$	→average surface salinity (psu)	Q_E	→latent heat of evaporation: (W m^{-2})
C	→cloudiness in tenths,	Q_H	→sensible heat flux: (W m^{-2})
C_H	→Stanton number: 10^{-3}	Q_L	→longwave heat flux: (W m^{-2})
c_p	→specific heat of moist air: 1010 ($\text{J kg}^{-1} \text{K}^{-1}$)	Q_{NET}	→net heat flux at the air-sea interface: (W m^{-2}),
c_{pw}	→ specific heat of the sea water: 3990 ($\text{J kg}^{-1} \text{°C}^{-1}$),	R	→correlation matrix of original variables
E	→diagonal eigenvalues matrix	S_{ver}	→vertical component of salt flux
E	→evaporated water mass (m s^{-1}),	T_a	→air temperature (°C),
F	→factor matrix of component loadings	T_w	→sea surface temperature (°C),
H_{ver}	→vertical component of the heat flux	$T_{w'}$	→sea surface temperature (K),
K_H	→vertical eddy diffusion coefficient of heat: ($\text{m}^2 \text{s}^{-1}$)	v	→wind speed (m s^{-1})
$k_k(i)$	→standardised PC scores	$x_k(i)$	→observed variables
		$y(t)$	→basic climatic oscillation
		$Y_z(t)$	→harmonic function
		$z_k(i)$	→standardised variables

Klimatske promjene i njihov utjecaj na oceanografske značajke Jadrana

Branka GRBEC

Institut za oceanografiju i ribarstvo, Split, Hrvatska

SAŽETAK

Istražen je utjecaj mogućih klimatskih promjena na oceanografska svojstva Jadrana. Analizirani su raspoloživi vremenski nizovi razine i površinske temperature mora, saliniteta i temperature mora na vertikalnom profilu srednjeg Jadrana. Moguće klimatske promjene pokušale su se odrediti analizom sekularnih meteoroloških nizova sa postaja na istočnoj obali Jadrana definiranjem osnovne klimatske oscilacije tlaka zraka, temperature zraka, oborine i razine mora. Rezultati su upućivali na činjenicu da, od atmosfere zavisni parametri u moru mogu pokazivati slične trendove, odnosno oscilacije. Stoga je tražena, na višegodišnjoj vremenskoj skali zavisnost promjena u moru od promjena u atmosferi. Pokušavajući objasniti glavne modove promjena u moru (opisanih metodom glavnih komponenata), uočeno je da su termohalina svojstava površinskog sloja, pod utjecajem atmosfere, i to znatnije u sjevernom nego južnom Jadranu. Intermedijalni sloj pod djelovanjem je dužjadranskog gradijenta tlaka zraka o čijoj veličini ovisi jačina ingresije. Na sezonskoj skali, osim što su određeni koeficijenti izmjene topline i soli u površinskom sloju, analizom promjena topline i soli odvojene su fizikalno dvije različite sezone: hladni dio godine s prevladavajućim vertikalnim procesima i topli dio godine s prevladavajućom horizontalnom advekcijom. Poznavajući procese koji na različitim vremenskim skalama mijenjaju svojstva mora, te uz pretpostavku dobivenih oscilacija i trendova u atmosferi, moguće je očekivati porast saliniteta cijelog vodenog stupca uzrokovanog smanjenjem oborine (površinski sloj) i porastom gradijenta tlaka zraka (intermedijarni sloj). Osim toga, uzrok porasta temperature mora, osim u sjevernom Jadranu, može biti posljedica horizontalnih, a ne vertikalnih procesa. Porast razine mora, posljedica je globalnih promjena, a ne lokalnih.

